Multi-Phase-Center Processing of POLARIS Data – Recent Results from Greenland and Antarctic Campaigns

D. Bekaert[(1)], N. Gebert[(1)], C.C. Lin[(1)], T. Casal[(1)], S.S. Kristensen[(2)], A. Kusk[(2)], J. Dall[(2)], S. López-Peña[(3)], J.F. Zurcher[(3)] and J. Mosig[(3)]

[(1)]ESA-ESTEC, Keplerlaan 1, PO Box 299, NL-2200 AG Noordwijk, the Netherlands
Tel: +31-71-5656086; E-mail: David.Bekaert@esa.int

[(2)]Technical University of Denmark, 2800 Kongens Lyngby, Denmark

[(3)]Swiss Fed. Inst. of Technology Lausanne, CH-1015 Lausanne, Switzerland

ABSTRACT

Radar ice sounding allows for the retrieval of ice depth and provides information on ice structures, flow, and layering. ESA's P-band POLarimetric Airborne Radar Ice Sounder (POLARIS) enables simultaneous reception of up to four individual channels. It has conducted campaigns over Greenland in 2008 and 2009 in a single aperture, polarimetric configuration [1] [2]. Results demonstrated the high sensitivity of POLARIS, enabling imaging of bedrock through ice sheet of more than 3000 m thickness, as shown in Fig. 1. Recently, POLARIS was upgraded with a larger antenna of 4 m length and during the 2011 spring campaign over Antarctica several datasets were acquired with this antenna in the multi-channel configuration. Such multi-phase centre antennas are essential for future space borne ice-sounding missions, as they enable the suppression of surface clutter returns that mask subsurface echoes.
This paper presents and investigates clutter suppression techniques and analyses their impact on the system performance based on the POLARIS configuration. Furthermore, preliminary surface clutter suppression results for the recently measured multi-channel data from Antarctica are presented, which were obtained with the ESA processor that is currently under development.

KEYWORDS: SAR, POLARIS, RADAR, P-BAND, ICE SOUNDING, CLUTTER SUPPRESSION, BEDROCK, ANTARTICA

INTRODUCTION

Understanding the role of the cryosphere in the climate change is one of the key elements of ESA's Living Planet programme [3]. In this context, radar ice sounding with its capability to provide three-dimensional characteristics of the major ice-sheets represents a very important tool, as this will improve the understanding of their history and possible future evolution through climate change.

Ice sounding from space

Radar ice sounding requires that the electromagnetic wave travels through thousands of meters of ice before being reflected from the underlying bedrock and received by the sensor. On the one hand, attenuation in ice is a crucial aspect, meaning that rather low radio frequencies are favourable for this application, as they exhibit a lower attenuation and penetrate deeper into the ice. As an example, current airborne sensors operate at carrier frequencies of 60 MHz or at 150 MHz [4] [5]. On the other hand, regions like Antarctica are not easily accessible by land and air due to the harsh environment, thus requiring significant funding for measurement campaigns. In perspective of ice sheet monitoring on a global scale, it will become necessary to perform measurements from a space borne platform, as this allows for regular imaging and illumination of a larger area on the ice surface. However, as the platform needs to fulfil the launcher constraints, limitations are imposed on the maximum antenna size. This means that in general higher frequencies are advantageous, as they allow for more compact antennas. This, however, is contradicting the ice sounding application, as high frequencies attenuate quicker in the ice. Additionally, the only frequency range allocated by ITU regulations is 435 MHz with a 6 MHz bandwidth.

It is for this reason that P-band represents a good compromise between antenna size and penetration depth. Nevertheless, at P-band, the surface clutter masking the subsurface echoes represents a major obstacle when operated from a satellite orbiting at an altitude of several hundreds of kilometres [5]. This asks for more sophisticated signal processing approaches, enabling surface clutter suppression [5], as will be detailed in the following.

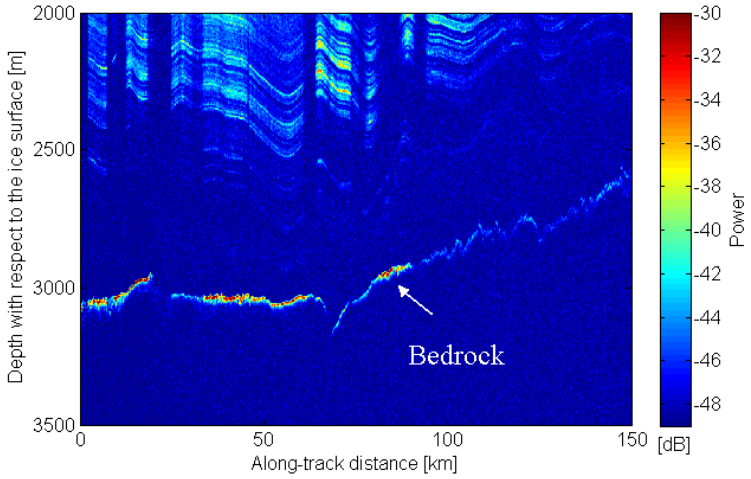

Fig. 1. POLARIS deep sounding result in Greenland

POLARIS

In 2008 and October 2009 ESA's P-band POLarimetric Airborne Radar Ice Sounder (POLARIS) was operated over Greenland in a single aperture, dual and polarimetric mode. The campaign conducted in 2009 included over-flights above the NEEM and NGRIP ice core drill-sites in directions parallel and orthogonal to the ice flow, allowing for studying the effects of the bi-refringence (ice crystal anisotropy). During these campaigns POLARIS proved its sensitivity, being able to image the bedrock through ice sheets of more than 3000 m depth, as is depicted in Fig. 1.
Later, POLARIS was enhanced with a larger antenna of 4 m length (initially this was 2 m), and still enabling simultaneous reception, digitization and storage of up to 4 channels after combination of two adjacent antenna elements each. Such a multi-phase centre configuration allows for post-processing techniques like surface clutter suppression. The upgraded POLARIS, for which the operational parameters and a schematic are respectively given in Table 1 and Fig. 2, was flown over Antarctica in spring 2011. This included overflights of the Antarctic Peninsula and Dronning Maud Land in East Antarctica, and above the EPICA drill-site at Kohnen Station.

Table 1: POLARIS parameters

Parameter	Value
Centre frequency	435 MHz
Wavelength in air	0.69 m
Transmitted bandwidths	85/30/6 MHz
Number of channels	4
Number of elements	8
Element spacing (wrt. centre)	0.48 m
Element length	0.408 m

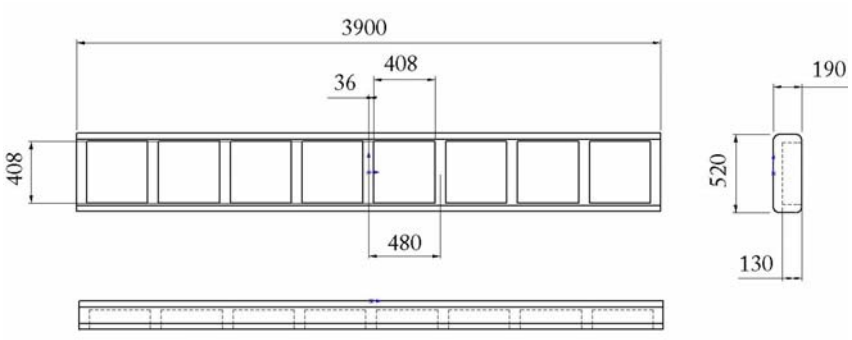

Fig. 2. Schematic of the POLARIS antenna, showing the 8 antenna elements arranged in across-track direction. Displayed dimensions are in mm.

SURFACE CLUTTER SUPPRESSION TECHNIQUES – OPTIMUM BEAMFORMER

As mentioned before, surface clutter can represent a major challenge to subsurface sounding. The radar transmits pulses and for each pulse, the radar measures on reception only the delay of the signal. Taking into account the flight altitude above ice, this delay can then be converted into an ice depth. This introduces an ambiguity to the system, as surface echoes from a specific off-nadir angle might exhibit a delay time identical to the sounding echo from a certain depth in nadir direction. Such ambiguous echoes are referred to as surface clutter sources. Assuming a flat ice surface topography and a nadir looking sensor, there are two ambiguous surface returns which are positioned symmetrically around nadir. However, in reality the sensor might be slightly rotated due to the rolling of the airplane and there will be topographic variations of the ice surface possibly introducing additional clutter sources at non-symmetric angles. A schematic representation of the clutter source geometry for an exemplary target P at depth R_{ice} is shown in Fig. 3, where θ_{nadir} and γ indicate the roll angle w.r.t the horizon and θ_n^i denotes the angle of arrival of the surface clutter echo from cell i. Further, H_{ice} gives the sensor height above the ice reference and deviations from this reference are denoted by dh. The identification of the surface clutter directions, i.e. the angles or arrival, can either be estimated from the data itself or can be computed by using a DEM of the ice topography. The first approach requires additional effort to estimate the direction of arrival from the data, but makes surface clutter cancellation independent from external auxiliary data [6]. The latter approach, which simply relies on an external DEM, is being implemented in our processor.

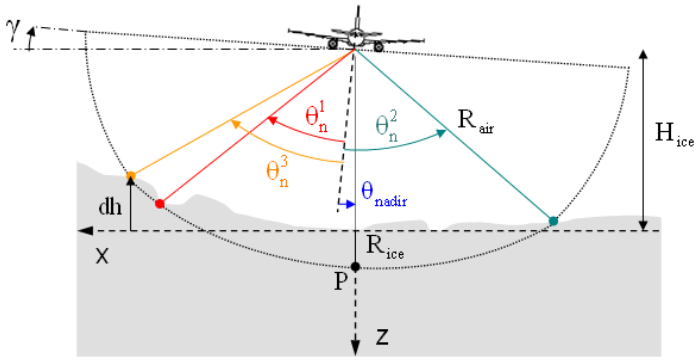

Fig. 3. Surface clutter sources

Based on the knowledge of the directions of arrival, the surface clutter can then be suppressed by applying a dedicated complex weight to each of the individual channels before forming the weighted sum of all channels. The two simplest cases of such a "digital beamforming" can be understood as follows:

a) First, one could think of simply steering the mainlobe of the joint receive antenna pattern always to nadir direction. Such **beam steering** achieved by applying a phase slope across the individual channels. This approach maximizes the signal power in a predefined direction, or, in other words, the thermal signal-to-noise ratio (SNR) is optimized. The drawback of this approach that it does do not account for the clutter at all.
b) Second, a so-called **null-steering** can be applied. This technique applies weights such that nulls are generated at specific angles of the joint antenna pattern, i.e. the clutter directions. Assuming perfect knowledge of the

topography, this leads to ideal suppression of clutter power, i.e. the optimum signal-to-clutter ratio (SCR). Forcing nulls in defined directions might lead to a mispointing of the antenna mainlobe away from nadir, thereby reducing the signal power. This means that the drawback of this technique is a possible degradation of the thermal SNR.

A globally optimum solution with respect to both thermal and clutter power is then given by a combination of the two above techniques. It is referred to as **optimum beamformer** in literature [7], with the weights of the individual channels chosen such that the joint power of thermal noise and clutter is minimized.
As derived in detail in [7], the respective weights can be calculated from (1), where the vector $\underline{w}$ contains the individual weights w_i for the channel i. The sensor geometry is represented by the array manifold vectors s_{nadir} and s_i. Basically, they describe the phase differences between the channels for a plane wave in the direction of interest, i.e. nadir, and the clutter sources, respectively. Taking into account the power of the clutter σ_i^2 in the specific directions (which can be interpreted as coloured noise) and thermal white noise of power σ_n^2, the covariance matrix R can be set up. One observes that R incorporates the clutter as coloured noise component and is additionally diagonally loaded according to the white noise. The optimum beamformer weights w are then computed by inverting this matrix as follows

$$\begin{aligned} \underline{w} &= R^{-1} s_{nadir} \\ R &= \sigma_n^2 \cdot I + \sum_{i=1}^{m} \sigma_i^2 s_i s_i^T \end{aligned}, \tag{1}$$

with I the identity matrix and σ_i^2/σ_n^2 being the clutter-to-noise ratio (CNR_i), which defines the ratio of thermal noise to clutter power. Illustratively, this ratio can be understood as the respective amount of beam-steering and null-steering in the final beamforming approach.
It should be noted that the antenna pattern itself already attenuates the clutter power for larger angles, and thus σ_i^2/σ_n^2 will depend on the angle. More specific, for larger angles the "natural" attenuation by the pattern becomes stronger and CNR decreases and, as a result, more focus can be put on the beam-steering.

As four receive channels are available, up to three echoes can be suppressed, i.e. m is bounded by N-1, with N defining the number of individual channels. This means that also a smaller number of suppressed directions can be chosen and finally this will underlie a trade-off, as will be explained in the following. E.g. in the case of three strong surface clutter echoes, the optimum strategy might be to suppress all three echoes, at the cost of thermal SNR. In this respect, the processor will be extended such that the local incidence angle, which strongly influences the backscattered power, will be considered. In specific, topographic information will be used to derive an estimate of the local incident angle and additionally consider this parameter to determine the three strongest echoes.
Different from suppressing the maximum possible number of strongest echoes, another possible strategy aims at suppression of only two clutter directions, which represents the "natural" case in flat topography. The benefit from such a strategy is automatically more importance is given to the optimization of the signal power. In illustrative words, instead of steering an additional null, the degree of freedom is used to steer the mainlobe to nadir thereby improving the thermal SNR.

SENSITIVITY ANALYSIS

As pointed out in the above section, both SNR and SCR depend on the chosen beamforming approach. As the thermal noise is assumed constant, variations in SNR and SCR are defined by variations of signal and clutter power. This section investigates the sensitivity of normalised signal power as well as normalised summed clutter power as it results from the different beamforming strategies. As input parameter for this analysis, the POLARIS parameters of Table 1 were used. In this context, it shall be highlighted that a number of 4 channels allows steering nulls to maximum three different directions. Furthermore, a mean altitude above ice of 3325 m was assumed, as this corresponds to the acquisition altitude of the measured data that will be presented in the following section.
In the case of the null-steering, two surface clutter cells are assumed and correspondingly two nulls are steered to the respective directions. Regarding the optimum beamformer, the same clutter source geometry is assumed, with a CNR of 40 dB.

The results are shown in Fig. 4, where Fig. 4 (a) depicts the normalised gain, which defines the signal power in dependency on the ice depth. Fig. 4 (b) shows the normalised summed gain responsible for the clutter power vs. ice

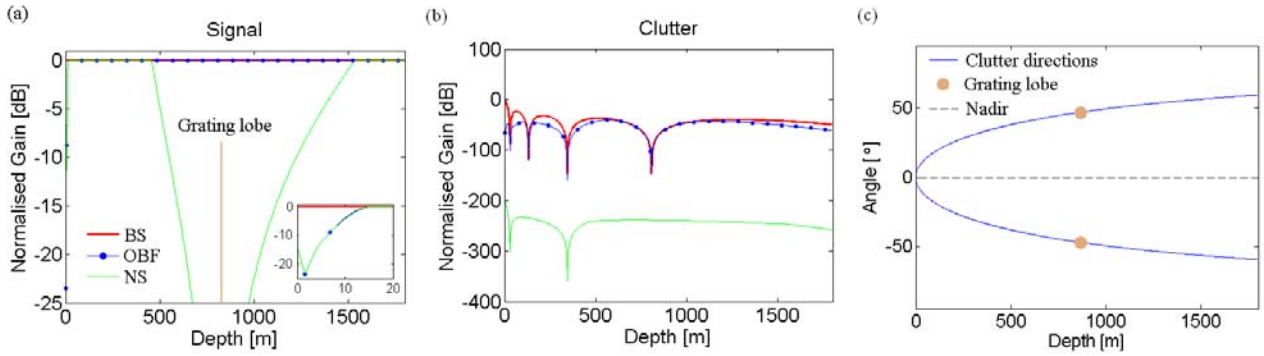

Fig. 4. Sensitivity analysis of the normalised signal gain (a), the normalised summed clutter gain (b) after applying beam-steering, null-steering and the optimum beamformer. The corresponding surface clutter directions (c), obtained assuming a flat topography, in absence of airplane roll, for an altitude of 3325 m and operational frequency of 435 MHz. The configuration assumed corresponds to the acquisition mode of the preliminary results shown below.

depth, while Fig. 4 (c) gives the relation between ice depth and clutter angle assuming a flat topography and no roll angle of the sensor.

Regarding the **signal power** in Fig. 4 (a), the optimum characteristic is represented by the beam steering ("BS", solid red line), which ensures a constant signal power vs. the ice depth. In contrast, the null-steering ("NS", solid green line) exhibits a dramatic loss of signal power around the depth that corresponds to the grating lobe. Please note that this results from the matrix which becomes singular for this case and thus the given example is only of theoretical nature but is no practical solution to the clutter suppression problem. More interesting is the result from the optimum beamformer ("OBF", dotted blue line), which guarantees nearly the same performance as the optimum beam steering for large depths. Only for very shallow depths up to 10 m a considerable loss of signal power is encountered, as shown by the integrated zoom in the lower right corner of Fig. 4 (a). This is caused by the fact that the surface clutter angle is within the antenna mainlobe; applying the clutter suppression in such a case inevitably results in a loss of signal power.

With respect to the **clutter power** in Fig. 4 (b), the beam steering ("BS", solid red line) exhibits clearly the worst suppression. This appears reasonable, as the weights do not aim at suppressing the clutter. In contrast, the optimum characteristic is represented by the null-steering ("NS", solid green line), which leads to a practically complete suppression of the clutter power. Being aware the presence of thermal noise, it becomes very clear that a suppression far below the thermal noise level is useless, as it will effectively not reduce the joint power of thermal noise and clutter. The important result of Fig. 4 (b) is represented by the optimum beamformer ("OBF", dotted blue line), which leads to a clearly improved suppression of clutter compared to the beam steering.

In conclusion, one can observe that the optimum beamformer represents a good compromise between clutter suppression and thermal SNR, as it ensures a clear reduction of the clutter power which comes at moderate cost of decreased signal power.

MEASURED DATA DEMONSTRATION OF SURFACE CLUTTER CANCELLATION - PRELIMINARY RESULTS

This section will present first results obtained from the data acquired in the 2011 Antarctica campaign. As the data was received very recently, it should be noted that the following results are preliminary and can only give first indications but not yet a demonstration of the full performance of the clutter suppression technique.

As a first step in the processing chain prior to clutter suppression, each channel is focussed separately. First, range compression is performed, followed by azimuth focussing. The latter is done by estimation of the phase history for a target at a specific depth and by applying a convolution of this estimate with the data. Only a limited part of the Doppler bandwidth is processed, such that range cell migration is avoided. Fig. 5 gives the azimuth and range compressed signal for each POLARIS channel, for a track over the Jutulstraumen glacier acquired in Antarctica during the 2011 campaign.

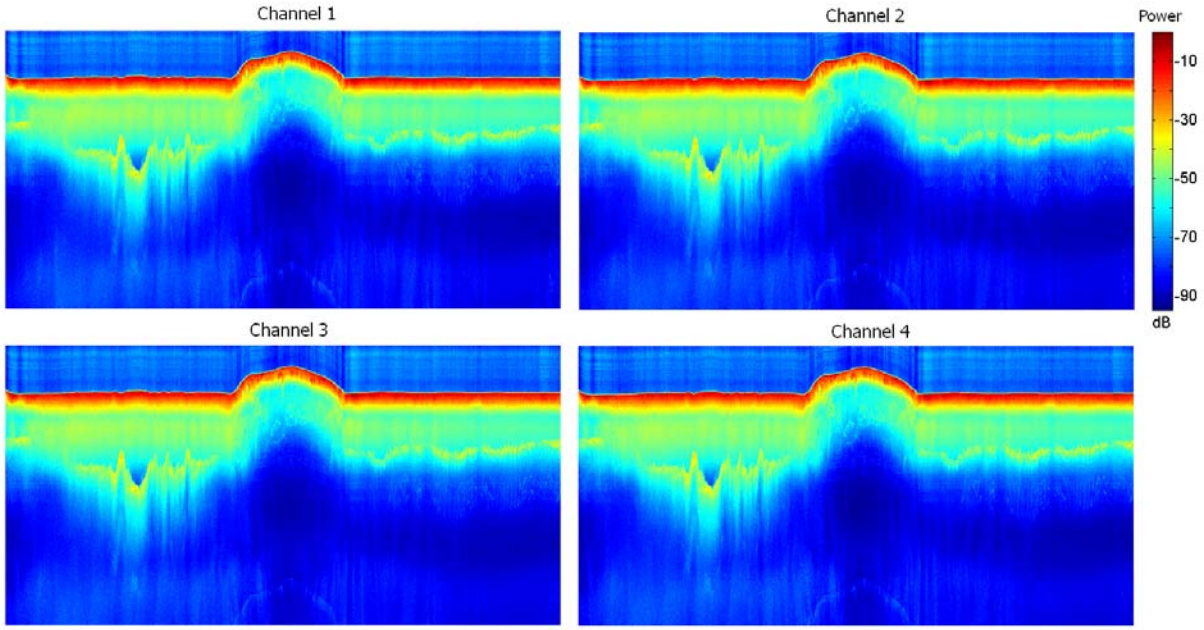

Fig. 5. Signal power for each of the four channels, each normalized with respect to its maximum surface return, for data acquired over the Jutulstraumen glacier, Antarctica**.**

In a next step, the clutter suppression algorithm, based on the optimum beamformer approach, is applied. As aforementioned, the processor is currently under development and thus the obtained results shall be considered preliminary. The algorithm relies on the airplane roll angle, as well on external ice topography data for estimation of the clutter source directions. As POLARIS has four receiving channels, it allows for suppression of up to three clutter directions. This introduces a trade-off in priority between the different clutter angles. In specific, the topography could be used to estimate the local incidence angle, and additionally consider this parameter to determine the three strongest echoes. However, in the current case of a rather flat topography it seems more favourable to suppress two rather than three clutter sources and benefit from in terms of the SNR, because one degree of freedom can be used to maximize the signal power in nadir [8].

As raw topography data is not yet processed, it is not included in our surface clutter location estimation. However, as aforementioned there is low variation of the ice topography for the Jutulstraumen glacier dataset (horizontal ice shelf), and thus it is valid to assume a flat surface across track. For simplicity, and due to low variation of the roll angle, we assume symmetric clutter sources about nadir, as depicted in Fig. 4 (c). The weighting coefficients were calculated for the optimum beamformer assuming a maximum CNR of 40 dB, which was scaled with the antenna pattern of a channel as it varies across the angle. The results for the weighted and combined channels are depicted in Fig. 6 on the right (“after clutter suppression”). The images are compared to the case where the four individual channels are simple added, i.e. a case that corresponds to a single receive antenna of larger size (“before clutter suppression”). All figures have as reference the maximum surface power in case no clutter correction is applied. For both scenarios, the figure depicts the complete scene (top) which clearly shows the strong (red) reflection of the ice surface but also clearly exhibits the bedrock, which is represented by the strong echo in the region of 500 – 800 m depth below the reference ice surface height. In addition, Fig. 6 bottom shows a zoom on two areas, which are marked in the global view with “1”and “2” and which are compared for the scenario with (grey frame) and without (red frame) clutter suppression. Zoom “1” concentrates on the surface return. One observes that the backscattered power close to the surface, which is represented by the extended red area, is clearly reduced by application of the clutter suppression. As will be explained in more detail below, this is on the one hand due to a reduction of surface clutter power, but on the other hand also partly caused by the reduced signal power.

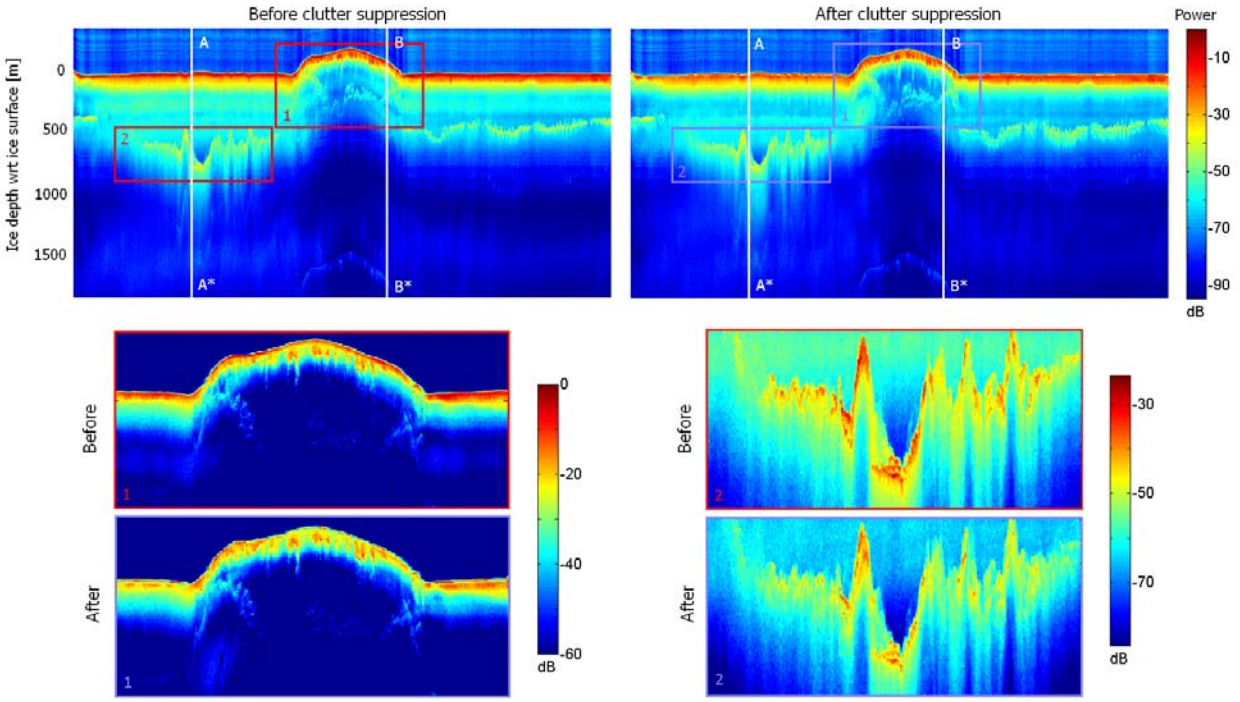

Fig. 6. Surface clutter suppression applied to flight over the Jutulstraumen glacier (horizontal ice shelf), preliminary results. Results show the power normalized with respect to the maximum surface return when no surface clutter correction has been applied. The strongest influence of surface clutter is observed for the shallower depths, as the signal from the surface is larger for smaller incidence angles.

The observation of reduced surface clutter is backed by the profiles along the cut AA*, which are depicted in Fig. 7, both for the case with (blue asterisks) and without clutter suppression (red circles). Fig. 7 top shows the region from the ice surface to a depth of 500 m. For example in the region from 180 m to 340 m depth (marked by the green ellipsoid), a clear reduction up to 10 dB of the backscattered clutter power can be observed when comparing the result after weighted combination of the multiple channels (blue) to the case when no clutter suppression is applied (red). Regarding the shallow depths directly below the surface (Fig.7, bottom), both clutter suppression as well as the aforementioned loss of signal power have to be taken into account. Recalling Fig. 4 a), an inevitable loss of signal power is observed up to 15 m depth (marked by the green rectangle) and this effect can be observed from the below

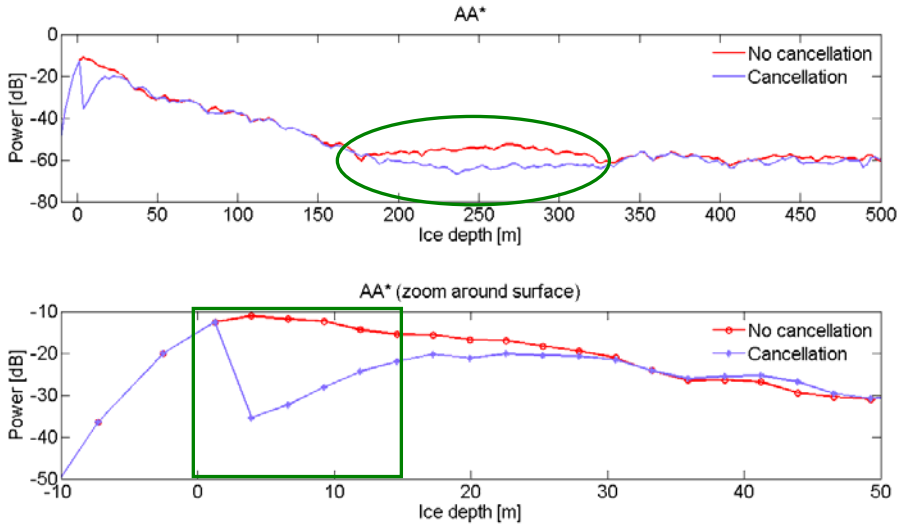

Fig. 7. Profile cuts along AA* ranging from the ice surface to 500 m depth (top) and a zoom on the first 50 m depth (bottom). Shown are the case with (blue) and without (red) application of surface clutter suppression.

profile, even in the same order of magnitude as predicted by Fig. 4. As a side remark, it should be mentioned that for the given antenna dimensions and these shallow depths, the optimum beamformer does not seem to represent the optimum solution and possibly another approach might be more favourable. Bu as all processing is performed a posteriori, this does not represent a problem, as for any depth an arbitrary processing approach can be chosen. For depths below 15 m, again a reduction of surface clutter can be seen. Please note that due to the preliminary character of these results, further investigations are needed, e.g. to clarify why no clutter reduction can be observed in the range from 30 to 180 m depth.

SUMMARY

The paper presented an overview of ESA's ESA's P-band POLarimetric Airborne Radar Ice Sounder (POLARIS) and its capability to detect the bedrock through more than 3000 m thick ice, as it was demonstrated with data acquired over Greenland. Furthermore, the importance of surface clutter suppression in the context of subsurface sounding radars was highlighted. Surface clutter cancellation requires systems with multiple receiving channels whose individual signals are then appropriately weighted and combined. Different strategies for such a "digital beamforming" were presented and a sensitivity analysis was performed, which investigated the impact of the different clutter suppression algorithms on performance parameters such as clutter and thermal noise power. The well-known "optimum beamformer" turned out to be the preferred solution, as this approach considers both thermal as well as clutter noise in an optimized way. Last but not least, multi-channel data acquired by POLARIS in the recent campaign over Antarctica has been processed and preliminary results for the clutter suppression have been presented.
As future work, a more detailed analysis of the multi-channel data will be carried out in order to quantify the performance of the different clutter suppression techniques and further confirm the validity of the theoretical sensitivity investigations. In this context, the ESA processor will be further developed and extended. For these results, the reader is referred to a submission for the upcoming EUSAR 2012 conference [8].

REFERENCES

[1] J. Dall, S.S. Kristensen, V. Krozer, C.C. Hernández, J. Vidkjær, A. Kusk, J. Balling, N. Skou, S.S. Søbjærg, E.L. Christensen, "ESA's polarimetric airborne radar ice sounder (POLARIS): Design and first results," *IET Radar, Sonar & Navigation*, vol. 4 (3), 2010.

[2] M. Villano, F. Hélière, C.C. Lin, P. Fabry, A. Kusk, "Synthetic Aperture Processing of Ice Sounding Radar Data: Results from POLARIS Test Campaign," *2nd Workshop on Advanced RF Sensors and Remote Sensing Instruments*, 16-18 Nov. 2009, Noordwijk, The Netherlands.

[3] Available online: http://www.esa.int/esaLP/ASE RBVNW9SC_index_0.html

[4] M. Peters, D. Blankenship, S. Carter, S. Kempf, D. Young, and J. Holt, "Along-Track Focusing of Airborne Radar Sounding Data From West Antarctica for Improving Basal Reflection Analysis and Layer Detection," *IEEE Trans. Geosc. & Rem. Sens.*, vol. 45 (9), Sep. 2007, pp. 2725-2736.

[5] K.C. Jezek, S. Gogineni, X. Wu, E. Rodriguez, F. Rodriguez-Morales, A. Hoch, A. Freeman, J.G. Sonntag, "Two-Frequency Radar Experiments for Sounding Glacier Ice and Mapping the Topography of the Glacier Bed," *IEEE Trans. Geosc. & Rem. Sens.*, vol. 49 (3), March 2011, pp.920-929.

[6] U. Nielsen, J. Dall, S.S. Kristensen, A. Kusk, "Coherent Surface Clutter Suppression Techniques with Topography Estimation for Multi-Phase-Center Radar Ice Sounding," *Proc. of EUSAR*, Nuremberg, Germany, April 2012, submitted.

[7] J.R. Guerci, "Space-Time Adaptive Processing", Artech House, 2003.

[8] D. Bekaert, N. Gebert, C.C. Lin, F. Hélière, J. Dall, A. Kusk, S.S. Kristensen, "Surface Clutter Suppression Techniques for P-band Multi-channel Synthetic Aperture Radar Ice Sounding," *Proc. of EUSAR*, Nuremberg, Germany, April 2012, submitted.

[9] N. Gebert, G. Krieger, and A. Moreira, "Digital Beamforming on Receive: Techniques and Optimization Strategies for High-Resolution Wide-Swath SAR Imaging," *IEEE Transactions on Aerospace and Electronic Systems*, vol. 45 (2), pp. 564-592, 2009.

[10] R. Scheiber, P. Prats, F. Hélière, "Surface Clutter Suppression Techniques for Ice Sounding Radars: Analysis of Airborne Data," *Proc. of EUSAR*, Friedrichshafen, Germany, June 2008.